

Article

# A Kinetic Study on the Efficient Formation of High-Valent Mn(TPPS)-oxo Complexes by Various Oxidants

Magdalena Prochner <sup>1,2</sup>, Łukasz Orzel <sup>2</sup>, Grażyna Stochel <sup>2</sup> and Rudi van Eldik <sup>2,3,\*</sup> 

<sup>1</sup> Jerzy Haber Institute of Catalysis and Surface Chemistry, Polish Academy of Sciences, Niezapominajek 8, 30-239 Kraków, Poland; magdalena.prochner@ikifp.edu.pl

<sup>2</sup> Faculty of Chemistry, Jagiellonian University, Gronostajowa 2, 30-387 Kraków, Poland; orzel@chemia.uj.edu.pl (Ł.O.); stochel@chemia.uj.edu.pl (G.S.)

<sup>3</sup> Department of Chemistry and Pharmacy, University of Erlangen-Nuremberg, Egerlandstr 1, 91058 Erlangen, Germany

\* Correspondence: rudi.vaneldik@fau.de; Tel.: +48-667772932

Received: 10 May 2020; Accepted: 27 May 2020; Published: 1 June 2020



**Abstract:** New, more efficient methods of wastewater treatment, which will limit the harmful effects of textile dyes on the natural environment, are still being sought. Significant research work suggests that catalysts based on transition metal complexes can be used in efficient and environmentally friendly processes. In this context, a number of compounds containing manganese have been investigated. A suitable catalyst should have the capacity to activate a selected oxidant or group of oxidants, in order to be used in industrial oxidation reactions. In the present study we investigated the ability of Mn<sup>III</sup>(TPPS), where TPPS = 5,10,15,20-tetrakis(4-sulphonatophenyl)-21H,23H-porphyrine, to activate five different oxidants, namely hydrogen peroxide, peracetic acid, sodium hypochlorite, potassium peroxomonosulfate and sodium perborate, via the formation of high valent Mn(TPPS)-oxo complexes. Kinetic and spectroscopic data showed that the oxidation process is highly pH dependent and is strongly accelerated by the presence of carbonate in the reaction mixture for three of the five oxidizing agents. The highest efficiency for the oxidation of Mn<sup>III</sup>(TPPS) to high-valent Mn(TPPS)-oxo complexes, was found for peracetic acid at pH  $\approx$  11 in 0.5 M carbonate solution, which is at least an order of magnitude higher than the rate constants found for the other tested oxidants under similar conditions.

**Keywords:** manganese(III) porphyrin; hydrogen peroxide; peracetic acid; sodium hypochlorite; potassium peroxomonosulfate; sodium perborate; oxidation processes

## 1. Introduction

Estimations concerning the amount of textile dyes that are discharged into water are quite different. Some articles state that 2% of the produced pigments are liberated in an aqueous effluent and the next 10% comes from the coloration process [1]. Other sources claim that 280,000 tons are released yearly [2]. This does not change the fact that the scale of the problem is huge. Especially, since insignificant amounts of dye may disrupt the water transparency, gas solubility and entail formation of toxic side products [2–5].

Due to the non-biodegradable character of dyestuffs and the possible release of toxic and carcinogenic byproducts, new methods for the degradation of dyes are still being sought [6–13]. New environmentally benign processes should reduce energy consumption and minimize the amount of chemicals, which are used in the overall cleaning operations. The alternative seems to be the application of catalysts based on transition metal complexes combined with oxidation agents in efficient

and environmentally friendly processes [14–16]. In this context a number of manganese complexes have been investigated [14,17,18].

The aforementioned approach requires the selection of adequate and harmless oxidants. One of the possible compounds is the well-known hydrogen peroxide. Besides its environmentally friendly nature,  $H_2O_2$  is cheap and the only by-products released during the oxidation process are water and molecular oxygen [19]. Moreover, other peroxides are also involved in industrial oxidation reactions. Potassium peroxomonosulfate (Oxone<sup>®</sup>) is mainly used in the degradation of organic pollutants in wastewater treatment due to its ability to produce sulfate radicals [20,21]. On the other hand, peracetic acid (PAA) is also one of the most commonly used green oxidants. PAA seems to have become one of the alternatives for chlorine and non-chlorine bleaching reagents [22]. Furthermore, the only side products that are formed are water and acetic acid. In the literature, a wide range of applications of PAA can be found. For decades, it was used in oxidation reactions of organic compounds [23] or as a disinfectant in medicine, the food industry and wastewater treatment [24–26]. In the context of industrial processes, two more oxidants are commonly used: sodium perborate (PBS) and sodium hypochlorite. PBS has been used for a long time especially in laundry cleaning [27]. In turn sodium hypochlorite is an inexpensive, strong oxidant, which has been used for years mostly as a bleaching and disinfectant agent. Beyond the indicated applications, NaOCl is widely used in epoxidation reactions of olefins [28–30], which are commonly catalyzed by transition metal complexes [31–36].

The aim of the present work was to examine the ability of selected Mn(III) porphyrin complexes to activate several, commonly used oxidants. This issue is extremely important within the context of possible application in degradation processes. The conducted studies covered the reactions of different oxidants with a commercially available sulfonated derivative of a Mn(III) porphyrin, referred to as Mn<sup>III</sup>(TPPS), where TPPS = 5,10,15,20-tetrakis(4-sulphonatophenyl)-21H,23H-porphyrine. Mn<sup>III</sup>(TPPS) has previously been used as a catalyst for the oxidation of olefins [37–39] and as a model catalyst in studies on monooxygenase or peroxidase activities [40], with various oxygen atom donors. Very good solubility in water, as well as the presence of side substituents that do not affect the course of the studied reactions, were decisive in the selection of this compound for our study.

In our earlier work, we investigated the activation of Mn<sup>III</sup>(TPPS) to form high valent oxo complexes using hydrogen peroxide [41,42]. In the present study we extended our studies to another four oxidants, namely peracetic acid, sodium hypochlorite, potassium peroxomonosulfate and sodium perborate. The studies allowed us to compare the efficiency of the formation of high-valent Mn(TPPS)-oxo complexes for the selected Mn<sup>III</sup>(TPPS)/oxidant systems under different, carefully selected conditions, and to select the most promising bleaching reagents for further studies. By improving our understanding of the kinetic and mechanistic aspects of these reactions, it should lead to a more structured approach to design highly efficient homogeneous catalysts.

## 2. Results

In this work, the oxidation reactions were carried out using a commercially available Mn<sup>III</sup>(TPPS) (see Figure 1a) porphyrin complex. The typical ultraviolet–visible (UV–Vis) spectrum of this complex can be described by the presence of a characteristic intense Soret band at 466 nm, two less intense bands at 379 and 401 nm, and weak Q bands at 564 and 596 nm (for a Mn<sup>III</sup>(TPPS) solution in water). Based on our previous studies, Mn<sup>III</sup>(TPPS) in aqueous solution has two pK<sub>a</sub> values (pK<sub>1</sub> = 6.6, pK<sub>2</sub> = 12.0) and hence can exist in three different forms, i.e., [Mn<sup>III</sup>(TPPS)(H<sub>2</sub>O)<sub>2</sub>]<sup>3-</sup>, [Mn<sup>III</sup>(TPPS)(H<sub>2</sub>O)(OH)]<sup>4-</sup> and [Mn<sup>III</sup>(TPPS)(OH)<sub>2</sub>]<sup>5-</sup>, depending on the pH of the solution [41]. Figure 1b shows how the pH affects the spectrum of Mn<sup>III</sup>(TPPS).

As shown in earlier studies, the oxidation of Mn<sup>III</sup>(TPPS) is connected with the hypsochromic shift of the most intense Soret band. The shift in the peak maximum from 466 nm to 422 nm is related to the formation of the high-valent (TPPS)Mn<sup>V</sup>=O species. On the other hand, the maximum at 402 nm is associated with the presence of (TPPS)Mn<sup>IV</sup>=O species [41]. Similar effects were also reported in the literature for other manganese porphyrin complexes [43–45].

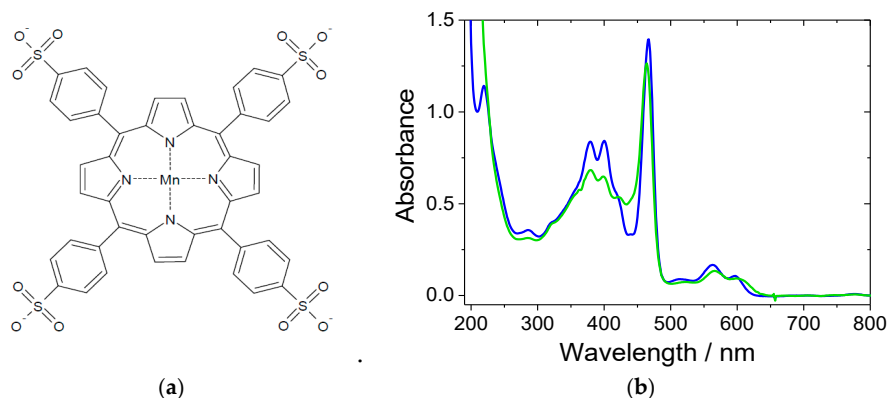


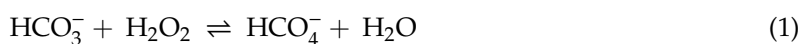
**Figure 1.** (a) Schematic structure of  $\text{Mn}^{\text{III}}(\text{TPPS})$ ; (b) ultraviolet–visible (UV–Vis) spectra of  $\text{Mn}^{\text{III}}(\text{TPPS})$  in water, pH = 7 (blue line) and in 0.01 M NaOH, pH = 12 (green line). Experimental conditions:  $[\text{Mn}^{\text{III}}(\text{TPPS})] = 12 \mu\text{M}$ ,  $T = 25 \text{ }^\circ\text{C}$ .

It was shown before that the formation of higher oxidation states of manganese is not efficient under acidic and neutral pH conditions due to the fact that the  $\text{Mn}^{\text{III}}(\text{TPPS})$  complex is mainly present in a more inert form with both axial positions occupied by water molecules. However, the application of more basic solutions, where one of the coordinated water molecules is replaced by a hydroxo ligand, leads to the fast oxidation of the porphyrin to form  $\text{Mn}(\text{IV})$ -oxo or  $\text{Mn}(\text{V})$ -oxo complexes [41]. The most efficient oxidation was observed at pH around 11 [42]. This maximum was ascribed to the *trans*-labilization of the coordinated water molecule by hydroxide in  $[\text{Mn}^{\text{III}}(\text{TPPS})(\text{H}_2\text{O})(\text{OH})]^{4-}$  and the very inert bishydroxo complex  $[\text{Mn}^{\text{III}}(\text{TPPS})(\text{OH})_2]^{5-}$ .

Based on this knowledge, we selected two pH values for which all spectroscopic and kinetic measurements were taken, namely pH 9.3 and 11. Also the careful selection of the type of buffer seemed to be essential. To prevent the unsuspected influence of buffer components on the kinetics of the scheduled reactions, we decided to follow the reactions in three types of solutions: in appropriately concentrated base, in 0.5 M solution of potassium nitrate (to keep the ionic strength at a constant level) with NaOH to adjust the pH, and in 0.5 M carbonate containing solution. Due to the fact that the oxidation of  $\text{Mn}^{\text{III}}(\text{TPPS})$  is too fast for using a standard UV–Vis spectrophotometer, all observed spectral changes and kinetic traces shown in this work were measured using the rapid-scan mode of a stopped-flow instrument.

Although the reactions of  $\text{Mn}^{\text{III}}(\text{TPPS})$  with  $\text{H}_2\text{O}_2$  were studied before, we decided to perform new measurements to obtain observed rate constants under the same conditions for all oxidants. This allowed us to compare the ability to oxidize  $\text{Mn}^{\text{III}}(\text{TPPS})$  by different oxidants. The results obtained for the reaction between  $\text{Mn}^{\text{III}}(\text{TPPS})$  and  $\text{H}_2\text{O}_2$  at pH = 9.3 and pH = 11 are presented in Figures S1 and S2 (Supporting Information).

At pH = 9.3 (Figure S1), the rate constants observed exhibit a linear dependence on the  $\text{H}_2\text{O}_2$  concentration with a significant intercept for Figure S1a and S1b. The intercept can be ascribed to a parallel decomposition reaction at low hydrogen peroxide concentration. The second-order rate constants are  $1.08 \pm 0.04$  (for Figure S1a),  $(3.2 \pm 0.2) \times 10^2$  (for Figure S1b) and  $(7.2 \pm 0.2) \times 10^3 \text{ M}^{-1} \text{ s}^{-1}$  (for Figure S1c), respectively. The highest value was obtained for the reaction in carbonate buffer, which is in good agreement with our previous studies [41,42]. The reaction in the presence of carbonate is usually much faster due to the rapid formation of the peroxocarbonate ion (percarbonate), according to Equation (1), which is a more powerful oxidizing agent than  $\text{H}_2\text{O}_2$  [46,47]. The equilibrium constant for this reaction is  $K = 0.32 \pm 0.02 \text{ M}^{-1}$  and the  $\text{p}K_{\text{a}}$  value for  $\text{HCO}_4^-/\text{CO}_4^{2-}$  is 10.6 [48,49].



In the case of measurements at pH = 11, also a linear dependence on hydrogen peroxide concentration was observed for reactions in NaOH and carbonate solutions (see Figure S2a,c). Both plots

show a considerable intercept, which is associated with decomposition reactions. The slope of the plots in Figure S2a,c represent the second-order rate constants, which are  $(2.20 \pm 0.06) \times 10^3$  and  $(9.3 \pm 0.7) \times 10^4 \text{ M}^{-1} \text{ s}^{-1}$  for Figure S2a,c, respectively.

The non-linear dependence of  $k_{\text{obs}}$  on the  $\text{H}_2\text{O}_2$  concentration observed in Figure S2b suggests that the reaction reaches a saturation level in terms of the observed rate constant. The second-order rate constant was taken from the initial slope and equals  $(4.1 \pm 0.7) \times 10^4 \text{ M}^{-1} \text{ s}^{-1}$ . Similar to  $\text{pH} = 9.3$ , the highest value was obtained for the reaction containing carbonate. It is worth noting that experiments at  $\text{pH} = 11$  show on average a one-order of magnitude higher rate constant than for the corresponding reactions at  $\text{pH} = 9.3$ . Due to the larger contribution of  $[\text{Mn}^{\text{III}}(\text{TPPS})(\text{H}_2\text{O})\text{OH}]^{4-}$  in solutions with increasing basicity, the manganese complex becomes more labile and can be more efficiently oxidized by  $\text{H}_2\text{O}_2$ ,  $\text{OOH}^-$  or  $\text{HCO}_4^-$ .

Subsequently, we used peracetic acid (PAA) instead of hydrogen peroxide to oxidize  $\text{Mn}^{\text{III}}(\text{TPPS})$ . PAA is produced in an equilibrium between hydrogen peroxide and acetic acid [50]. The reaction is catalyzed by sulfuric acid and proceeds according to Equation (2):



Due to this equilibration reaction, it is obvious that PAA solutions contain a certain concentration of  $\text{H}_2\text{O}_2$ . In the literature it is postulated that both peroxides are strong oxidants. On comparing PAA and  $\text{H}_2\text{O}_2$ , an advantage of the former is its lower tendency to undergo catalase reactions. Participation of the oxidants in catalase reactions causes faster decomposition of the oxidant and could be a problem in efficient degradation processes catalyzed by transition metal complexes [22,51]. Detailed spectroscopic and kinetic studies were performed to follow the oxidation of  $\text{Mn}^{\text{III}}(\text{TPPS})$  by PAA at  $\text{pH} 9.3$  and 11. Typical spectral changes and a kinetic trace are shown in Figure 2.

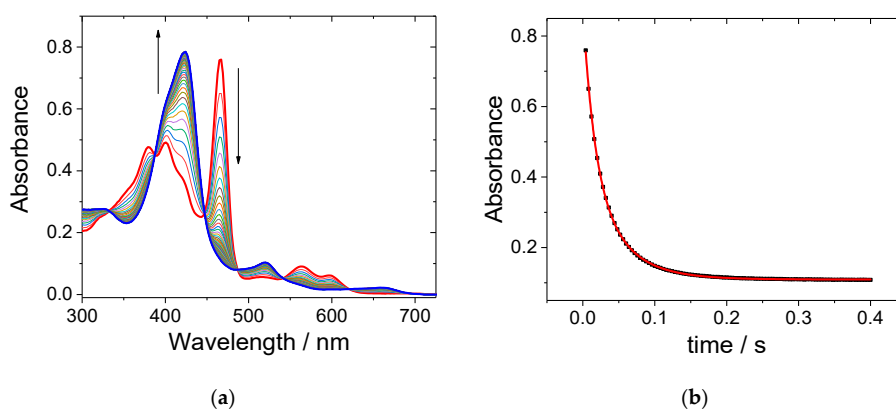


**Figure 2.** (a) Spectral changes recorded during the reaction of  $\text{Mn}^{\text{III}}(\text{TPPS})$  and peracetic acid (PAA) at  $\text{pH} = 11$  in the presence of carbonate in solution. Spectrum just after mixing the reactants (red line) and after 0.4 s (blue line); (b) typical kinetic trace recorded at 466 nm. Experimental conditions:  $[\text{Mn}^{\text{III}}(\text{TPPS})] = 6 \mu\text{M}$ ,  $[\text{PAA}] = 50 \mu\text{M}$ ,  $[\text{Na}_2\text{CO}_3 + \text{NaHCO}_3] = 0.5 \text{ M}$ ,  $T = 25 \text{ }^\circ\text{C}$ , total reaction time = 0.4 s.

Upon addition of PAA to a solution of  $\text{Mn}^{\text{III}}(\text{TPPS})$  in basic aqueous media, an immediate decrease in the absorption of the Soret band at 466 nm was observed (see Figure 2a). Simultaneously, a new broad band at 422 nm was formed. The observed hypsochromic shift is ascribed to the oxidation of  $\text{Mn}^{\text{III}}(\text{TPPS})$  to  $(\text{TPPS})\text{Mn}^{\text{V}}=\text{O}$  as described above. The formation of  $\text{Mn}^{\text{V}}=\text{O}$  species was completed in less than 0.4 s and revealed clean isosbestic points at 387, 447, 487 and 542 nm. The overall observed spectral changes are in good agreement with our earlier work dealing with the  $\text{Mn}^{\text{III}}(\text{TPPS})/\text{H}_2\text{O}_2$  system. A typical kinetic trace presented in Figure 2b shows very good pseudo-first order behavior and can be fitted satisfactory with a single exponential function.

To gain more information on the reactivity of  $\text{Mn}^{\text{III}}(\text{TPPS})$  with PAA, we conducted experiments with different concentrations of PAA at pH = 9.3 and pH = 11. The obtained results are shown in Figure 3 and Figure S3.

Plots of the observed rate constants vs.  $[\text{PAA}]$  in Figure 3a and Figure S3a exhibit a linear dependence with an almost unnoticeable intercept. The small intercept can be ascribed to a parallel decomposition of the porphyrin complex that occurs at low PAA concentrations. The obtained second-order rate constants for these reactions at pH 9.3 in carbonate solution (Figure 3a) and at pH 11 in basic solution (Figure S3a) are  $(1.26 \pm 0.02) \times 10^5 \text{ M}^{-1} \text{ s}^{-1}$  and  $(2.19 \pm 0.06) \times 10^4 \text{ M}^{-1} \text{ s}^{-1}$  at 25 °C, respectively. It differs for plots recorded at pH = 11 in solutions containing  $\text{KNO}_3$  and carbonate. For these plots, the data exhibit saturation kinetics (see Figure S3b and Figure 3b). The second-order rate constants were taken from the initial slope and equal  $(9.3 \pm 2.0) \times 10^4 \text{ M}^{-1} \text{ s}^{-1}$  and  $(1.7 \pm 0.4) \times 10^6 \text{ M}^{-1} \text{ s}^{-1}$ , respectively. As in the case of the hydrogen peroxide system, the higher value was found for the reaction at pH = 11 in the presence of carbonate in solution. However, a comparison of all the values found for  $\text{H}_2\text{O}_2$  as oxidant, with those obtained for the same reaction with PAA, leads to the conclusion that the efficiency of the formation of high-valent  $\text{Mn}(\text{TPPS})$ -oxo complexes by PAA is significantly higher by an order of magnitude in terms of the second-order rate constant. This suggests that PAA is a more efficient oxidant in comparison to  $\text{H}_2\text{O}_2$  under the selected conditions. Moreover, kinetic data showed that the oxidation by PAA is accelerated in carbonate solution. This can be accounted for in terms of the formation of peroxocarbonate in the presence of  $\text{H}_2\text{O}_2$ , which is released by the hydrolysis of PAA according to Equation (2).

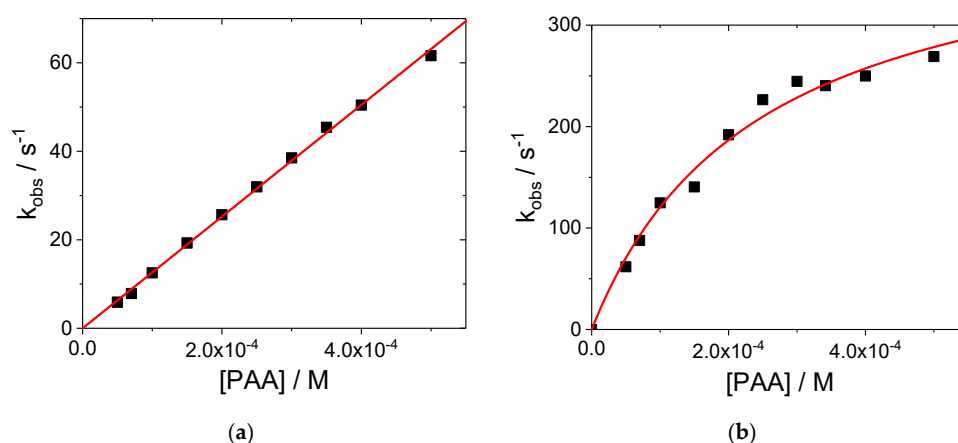


**Figure 3.** Plot of  $k_{\text{obs}}$  versus PAA concentration for the reaction of  $\text{Mn}^{\text{III}}(\text{TPPS})$  with PAA: (a) at pH = 9.3 in carbonate buffer; (b) at pH = 11 in 0.5 M  $\text{Na}_2\text{CO}_3 + \text{NaHCO}_3$  solution. Experimental conditions:  $[\text{Mn}^{\text{III}}(\text{TPPS})] = 6 \mu\text{M}$ ,  $[\text{PAA}] = 50\text{--}500 \mu\text{M}$ ,  $T = 25 \text{ }^\circ\text{C}$ .

It should be underlined that for pH = 9.3 only the reactions in the presence of carbonate buffer were successfully measured. Reactions in basic and  $\text{KNO}_3$  solution showed low reproducibility and were not taken into consideration. It is suggested in the literature that PAA itself can undergo three potential reactions, namely hydrolysis to  $\text{H}_2\text{O}_2$  and acetic acid, spontaneous decomposition, and decomposition catalyzed by transition metal ions. These reactions may have an effect on the complexity of the observed processes and cause insufficient reproducibility of results especially at a pH close to the  $\text{pK}_a$  value of PAA, which is 8.2 [22,51–55].

In a next step, we extended our work to elucidate how  $\text{Mn}^{\text{III}}(\text{TPPS})$  reacts with sodium hypochlorite.  $\text{NaOCl}$  exists in aqueous solution as an equilibrium between hypochlorous acid ( $\text{HOCl}$ ) and hypochlorite ion ( $\text{OCl}^-$ ) at pH 5–10 [56]. The  $\text{pK}_a$  value of  $\text{HOCl}$  is 7.53 [57]. Sodium hypochlorite undergoes an un-catalyzed two-step decomposition according to the reactions in Equations (3) and (4) [58]:



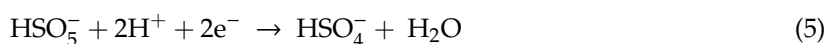


In the work by Lister it was shown that the reaction described in Equation (3) is the rate-determining slow step with the larger activation energy barrier. Moreover, the influence of sodium hydroxide, carbonate and chloride on the stability of NaOCl was studied. The data showed that the mentioned compounds do not exert a catalytic effect on the reactions outlined in Equations (3) and (4) [58].

A series of measurements between  $\text{Mn}^{\text{III}}(\text{TPPS})$  and NaOCl at pH 9.3 and 11 were conducted. Monitoring of the kinetic traces at 466 nm, which mostly showed very good pseudo-first order behavior, allowed the kinetic data shown in Figures S4 and S5 to be obtained. However, for the reaction at pH = 9.3 in base, it was necessary to fit the kinetic traces with a double exponential function. This effect was probably due to the unstable pH value during measurements, which was caused by the presence of only a diluted basic solution in the test system. Calculated rate constants exhibited a linear dependence on the NaOCl concentration. Only for pH = 9.3 with  $\text{KNO}_3$  (see Figure S4b) and pH = 11 with base (see Figure S5a), a significant intercept was observed. It can be associated with the back reaction in which  $(\text{TPPS})\text{Mn}^{\text{V}}=\text{O}$  is reduced to the initial  $\text{Mn}^{\text{III}}(\text{TPPS})$  in a parallel reaction. The slope of the plots in Figures S4 and S5 represent the second-order rate constants for the oxidation of  $\text{Mn}^{\text{III}}(\text{TPPS})$ , which are  $(4.1 \pm 0.2) \times 10^2$ ,  $(1.42 \pm 0.07) \times 10^3$  and  $(1.46 \pm 0.04) \times 10^3 \text{ M}^{-1} \text{ s}^{-1}$  for pH = 9.3 and  $(9.6 \pm 0.4) \times 10^2$ ,  $(3.65 \pm 0.06) \times 10^3$  and  $(1.19 \pm 0.03) \times 10^4 \text{ M}^{-1} \text{ s}^{-1}$  for pH = 11, respectively.

Analysis of the second-order rate constants for the oxidation of  $\text{Mn}^{\text{III}}(\text{TPPS})$  by NaOCl to form high-valent  $\text{Mn}(\text{TPPS})$ -oxo complexes, indicates that the process is favored at pH  $\approx 11$ . Furthermore, the reported rate constants are insignificantly higher than those for the  $\text{Mn}^{\text{III}}(\text{TPPS})/\text{H}_2\text{O}_2$  system. However, they are lower than those obtained for the  $\text{Mn}^{\text{III}}(\text{TPPS})/\text{PAA}$  system. This suggests that NaOCl is a more efficient oxidant than  $\text{H}_2\text{O}_2$ , but a less efficient oxidant than PAA for the studied oxidation process. Moreover, the presence of carbonate in the solution has insignificant influence on the second-order rate constants. This demonstrates that the presence of carbonate does not affect the oxidation process as it was in the case for the  $\text{Mn}^{\text{III}}(\text{TPPS})/\text{H}_2\text{O}_2$  and  $\text{Mn}^{\text{III}}(\text{TPPS})/\text{PAA}$  systems.

To gain more information about the reactions between  $\text{Mn}^{\text{III}}(\text{TPPS})$  and potassium peroxomonosulfate or sodium perborate, more detailed measurements using the rapid-scan mode of a stopped-flow instrument were conducted. Potassium peroxomonosulfate is commercially available as the stable triple salt  $\text{KHSO}_5 \cdot 0.5 \text{KHSO}_4 \cdot 0.5 \text{K}_2\text{SO}_4$  (Oxone<sup>®</sup>). Oxone is non-toxic and has good water solubility. The  $\text{pK}_a$  value of  $\text{HSO}_5^-/\text{SO}_5^{2-}$  is 9.4. It is commonly used in synthesis and oxidation of organic compounds (such as alkenes, aldehydes, ketones, phenols) [59] and as an efficient disinfectant. The peroxomonosulfate anion ( $\text{HSO}_5^-$ ) is a relatively strong oxidant with a standard electrode potential of 1.82 V (vs. NHE) according to Equation (5) [60]:

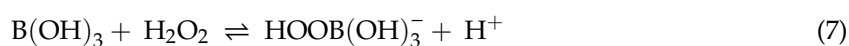


The peroxomonosulfate ion requires activation by transition metals, or irradiation, for the efficient degradation of pollutants. Activated  $\text{HSO}_5^-$  can easily generate sulfate radicals [60].

The perborate anion is produced when in aqueous solution boric acid and hydrogen peroxide are mixed together [61]. The  $\text{pK}_a$  of boric acid is 8.98 [62], which indicates that above pH 9 the borate anion predominates according to Equation (6) with  $K_{(\text{BOH})_3} = 1.0 \times 10^{-9} \text{ M}$ .



In the presence of hydrogen peroxide, boric acid exists in equilibrium with two other forms, namely monoperoxoborate (also called perborate) and diperoxoborate ions, as shown below in Equations (7) and (8) with equilibrium constants  $K_{\text{HOOB}(\text{OH})_3^-} = 2.0 \times 10^{-8}$  and  $K_{(\text{HOO})_2\text{B}(\text{OH})_2^-} = 2.0 \text{ M}^{-1}$  [63]:



It is suggested in the literature that peroxoborate is the main species in the pH range 7–13, however, this depends on the concentrations of borate and hydrogen peroxide in solution. It is postulated that perborate is more reactive than percarbonate, but less reactive than persulfate and peroxy-carboxylic acids [61,63,64]. The results of our kinetic studies dealing with the interactions between  $Mn^{III}(TPPS)$  and persulfate or perborate are presented in Figures S6 and S7. All results were obtained using the stopped-flow technique.

It is worth noting that reproducible results were obtained only for measurements at pH = 11. The dependence of the determined  $k_{obs}$  values on the peroxomonosulfate concentration in potassium nitrate solution (see Figure S6a) exhibits saturation kinetics with a second-order rate constant of  $(4.4 \pm 1.1) \times 10^4 M^{-1} s^{-1}$  calculated from the initial slope of the plot. It is different in carbonate-containing solution (see Figure S6b), where  $k_{obs}$  exhibits a linear dependence on the peroxomonosulfate concentration with a second-order rate constant  $(1.17 \pm 0.02) \times 10^5 M^{-1} s^{-1}$ . All kinetic traces showed very good pseudo-first order behavior and could be fitted with a single exponential function. Similarly, when perborate was used, plots of  $k_{obs}$  versus perborate concentration are linear with a small intercept in Figure S7b, which is probably associated with a slow parallel decomposition of the catalyst that cannot be avoided. The second-order rate constants obtained were  $(8.8 \pm 0.2) \times 10^2 M^{-1} s^{-1}$  and  $(3.7 \pm 0.2) \times 10^4 M^{-1} s^{-1}$ , respectively. It should be underlined that the presence of carbonate in solution significantly accelerates the reaction with perborate. This is probably due to the fact that perborate is always in equilibrium with an appropriate amount of hydrogen peroxide, which is able to rapidly generate the percarbonate ion in the reaction with carbonate as described earlier. In the case of persulfate, the difference between the rate of the reaction with and without carbonate was much smaller.

For clarity, all obtained values of second-order rate constants are collected in Table 1.

**Table 1.** Rate constants for the oxidation of  $Mn^{III}(TPPS)$  by studied oxidants at 25 °C.

Oxidant	Experimental Conditions	Second-Order Rate Constant $M^{-1} s^{-1}$
$H_2O_2$	pH = 9.3, NaOH	$1.08 \pm 0.04$
	pH = 9.3, 0.5 M $KNO_3$ + NaOH	$(3.2 \pm 0.2) \times 10^2$
	pH = 9.3, 0.5 M $NaHCO_3$ + $Na_2CO_3$	$(7.2 \pm 0.2) \times 10^3$
	pH = 11, NaOH	$(2.20 \pm 0.06) \times 10^3$
	pH = 11, 0.5 M $KNO_3$ + NaOH	$(4.1 \pm 0.7) \times 10^4$ <sup>[a]</sup>
	pH = 11, 0.5 M $NaHCO_3$ + $Na_2CO_3$	$(9.3 \pm 0.7) \times 10^4$
PAA	pH = 9.3, 0.5 M $NaHCO_3$ + $Na_2CO_3$	$(1.26 \pm 0.02) \times 10^5$
	pH = 11, NaOH	$(2.19 \pm 0.06) \times 10^4$
	pH = 11, 0.5 M $KNO_3$ + NaOH	$(9.3 \pm 2.0) \times 10^4$ <sup>[a]</sup>
NaOCl	pH = 11, 0.5 M $NaHCO_3$ + $Na_2CO_3$	$(1.7 \pm 0.4) \times 10^6$ <sup>[a]</sup>
	pH = 9.3, NaOH	$(4.1 \pm 0.2) \times 10^2$
	pH = 9.3, 0.5 M $KNO_3$ + NaOH	$(1.42 \pm 0.07) \times 10^3$
	pH = 9.3, 0.5 M $NaHCO_3$ + $Na_2CO_3$	$(1.46 \pm 0.04) \times 10^3$
	pH = 11, NaOH	$(9.6 \pm 0.4) \times 10^2$
	pH = 11, 0.5 M $KNO_3$ + NaOH	$(3.65 \pm 0.06) \times 10^3$
peroxomonosulfate	pH = 11, 0.5 M $NaHCO_3$ + $Na_2CO_3$	$(1.19 \pm 0.03) \times 10^4$
	pH = 11, 0.5 M $KNO_3$ + NaOH	$(4.4 \pm 1.1) \times 10^4$ <sup>[a]</sup>
perborate	pH = 11, 0.5 M $NaHCO_3$ + $Na_2CO_3$	$(1.17 \pm 0.02) \times 10^5$
	pH = 11, 0.5 M $KNO_3$ + NaOH	$(8.8 \pm 0.2) \times 10^2$
	pH = 11, 0.5 M $NaHCO_3$ + $Na_2CO_3$	$(3.7 \pm 0.2) \times 10^4$

<sup>[a]</sup> Taken from the initial slope of the plots in Figure S2b, Figure 3b and Figure S3b.

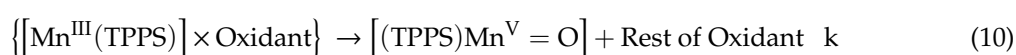
### 3. Discussion

In this study it was our aim to investigate the ability of  $Mn^{III}(TPPS)$  to react with commercially available oxidants to form high-valent  $Mn(TPPS)$ -oxo complexes as catalytic active species in an

efficient way. We examined five different oxidants, *viz.* hydrogen peroxide, peracetic acid, sodium hypochlorite, potassium peroxomonosulfate and sodium perborate, in their reactions with  $\text{Mn}^{\text{III}}(\text{TPPS})$ . Although we studied the interaction of  $\text{Mn}^{\text{III}}(\text{TPPS})$  with  $\text{H}_2\text{O}_2$  before, we repeated these measurements under the same conditions as for the other oxidants. It allowed us to minimize the influence of pH changes and small differences in the constitution of solutions between experiments with hydrogen peroxide and the remaining oxidants. The results showed that the second-order rate constants for the formation of high-valent  $\text{Mn}(\text{TPPS})$ -oxo complexes are similar for the three oxidants: hydrogen peroxide, sodium hypochlorite and sodium perborate. Overall, significantly higher second-order rate constants were obtained for peracetic acid and potassium peroxomonosulfate. The most efficient formation of high-valent  $\text{Mn}(\text{TPPS})$ -oxo complexes was found for PAA at  $\text{pH} \approx 11$  in carbonate solution, which is at least an order of magnitude higher than for the other tested oxidants on the basis of the reported second-order rate constants. It can be concluded that peracetic acid is the most efficient oxidant of  $\text{Mn}^{\text{III}}(\text{TPPS})$  among all tested oxidants under the selected conditions.

It is worth noting that the formation of higher oxidation state  $\text{Mn}(\text{TPPS})$ -oxo species is faster and favored at  $\text{pH} = 11$ . This is due to the presence of the  $\text{Mn}^{\text{III}}(\text{TPPS})$  complex more in the  $[\text{Mn}^{\text{III}}(\text{TPPS})(\text{H}_2\text{O})\text{OH}]^{4-}$  form than in the  $[\text{Mn}^{\text{III}}(\text{TPPS})(\text{H}_2\text{O})_2]^{3-}$  form, which is more labile as a result of the *trans*-labilization by the hydroxo ligand and therefore more reactive. Our studies also revealed that carbonate in solution significantly accelerated the reactions with  $\text{H}_2\text{O}_2$ , PAA and perborate. As shown before, in basic aqueous solutions containing carbonate and hydrogen peroxide, the rapid formation of peroxocarbonate ( $\text{HCO}_4^-$ ) is observed. It is postulated that peroxocarbonate is a stronger oxidant than hydrogen peroxide and thus can easier oxidize  $\text{Mn}^{\text{III}}(\text{TPPS})$ . Due to the fact that peracetic acid and perborate are always in an equilibrium with  $\text{H}_2\text{O}_2$ , also in basic solutions,  $\text{HCO}_4^-$  ions can be formed.

In some cases the plots of  $k_{\text{obs}}$  versus oxidant concentration reached a limiting value (saturation kinetics, see Figure S2b, Figure 3b and Figure S3b) which can be ascribed to rapid precursor formation (K) between a specific  $\text{Mn}^{\text{III}}(\text{TPPS})$  complex and the oxidant as shown in Equations (9) and (10), followed by the rate-determining (k) formation of the high valent  $\text{Mn}^{\text{V}}=\text{O}$  oxo complex. Subsequently, the high-valent oxo complex oxidizes the substrate (S) in a fast reaction to reform the  $\text{Mn}^{\text{III}}(\text{TPPS})$  complex (to complete the catalytic cycle) and the oxidized substrate (SO) as shown in Equation (11).



Based on the mechanism outlined in Equations (9) to (11) for oxidant in excess, the observed first-order rate constant can be expressed as Equation (12),

$$k_{\text{obs}} = kK[\text{Oxidant}] / \{1 + K[\text{Oxidant}]\} \quad (12)$$

which simplifies to  $k_{\text{obs}} = kK$  [oxidant] at low [oxidant], and  $k_{\text{obs}} = k$  at high [oxidant]. Thus, the initial slope of the curved concentration dependence represents  $kK$ , i.e., the second-order rate constant, and the maximum rate constant reached at saturation represents  $k$ , the rate-determining step of the suggested reaction mechanism.

Finally, it can be concluded that, in the longer term, the results presented in this work may have a positive impact on the design of new, efficient and environmentally friendly catalytic systems, which can be used in industrial processes for the purification of wastewater.

#### 4. Materials and Methods

All chemicals were of analytical grade and used without further purification. Pure sodium hydroxide micro-pills and hydrochloric acid were provided by POCH (Avantor Performance Materials Poland S.A., Gliwice, Poland).  $\text{Mn}^{\text{III}}(\text{TPPS})\text{Cl}$ , where TPPS = 5,10,15,20-tetrakis(4-sulphonatophenyl)-21H,23H-porphyrin, sodium carbonate, sodium hydrogen carbonate, peracetic acid, sodium hypochlorite, sodium perborate, Oxone<sup>®</sup> and potassium nitrate, were supplied by Sigma–Aldrich (Merck KGaA, Darmstadt, Germany). Hydrogen peroxide (30% w/w) was purchased from Chempur (Chempur, Piekary Śląskie, Poland). The concentration of  $\text{H}_2\text{O}_2$  was determined by standard titration with  $\text{KMnO}_4$  in an acidic medium. Water used in all the experiments was distilled and deionized (Mili-Q system).

The time-resolved visible spectra were recorded on a SX20 (Applied Photophysics, Leatherhead, Surrey, UK) stopped-flow spectrophotometer using a rapid scan photodiode array mode with 1 nm spectral resolution. The temperature was controlled by a Labo Plus, Polyscience (Labo Plus sp. Z o.o., Warsaw, Poland) thermostat bath. All measurements were done at 25 °C. One syringe of the stopped-flow instrument was filled with the  $\text{Mn}^{\text{III}}(\text{TPPS})$  complex and the second one with the appropriate oxidant solution. Both solutions were at the chosen pH. In the experiments dealing with the kinetics of the reactions, the traces were followed at 466 nm. Complete spectra and single wavelength kinetic traces were collected. Data were processed using the Pro-Data and OriginPro 2019 software. The pH measurements were carried out with a HI 221 (HANNA Instruments Polska, Olsztyn, Poland) pH-meter combined with a Hydromet ERH-13–6 electrode (Hydromat, Gliwice, Poland). The pH-meter was calibrated for two points with standard buffer solutions at pH 7, 9, 10 and 12.46, depending on the pH range required.

All solutions were freshly prepared before use by dissolving the starting material in pure, distilled water. Concentrations of  $\text{Mn}^{\text{III}}(\text{TPPS})$  were evaluated spectroscopically based on the absorption coefficients determined at different pH values. Different carbonate or NaOH solutions were used to adjust the pH of the experimental solutions. Carbonate buffer at pH 9.3 was prepared by dissolving and mixing  $\text{NaHCO}_3$  with  $\text{Na}_2\text{CO}_3$  in water. For pH 11, dissolved  $\text{Na}_2\text{CO}_3$  with the addition of NaOH was used. Sodium hydroxide solutions were obtained by dissolving suitable amounts of NaOH. In some cases,  $\text{KNO}_3$  was used to control the ionic strength. All reported concentrations are the final values obtained after mixing and dilution of the reactants.

#### 5. Conclusions

The results presented in this paper indicate that  $\text{Mn}^{\text{III}}(\text{TPPS})$  can easily be activated by a wide range of oxidants to form a promising catalyst for many different oxidation reactions. We have shown that hydrogen peroxide, peracetic acid, sodium hypochlorite, potassium peroxomonosulfate and sodium perborate can oxidize  $\text{Mn}^{\text{III}}(\text{TPPS})$  to form high-valent Mn(V)-oxo species under appropriate conditions. All studied systems show high second-order rate constants for the formation of Mn(V)-oxo species. The highest value was found for the  $\text{Mn}^{\text{III}}(\text{TPPS})/\text{PAA}$  system at  $\text{pH} \approx 11$  in carbonate solution, which indicates that peracetic acid is the most efficient oxidant under the selected conditions. Moreover, it can be concluded that for all tested systems the oxidation of  $\text{Mn}^{\text{III}}(\text{TPPS})$  is much faster at  $\text{pH} = 11$  compared to  $\text{pH} = 9.3$ , which is due to the presence of the most labile form of  $\text{Mn}^{\text{III}}(\text{TPPS})$ , viz.  $[\text{Mn}^{\text{III}}(\text{TPPS})(\text{H}_2\text{O})(\text{OH})]^{4-}$ . It is worth noting that the use of carbonate solutions significantly accelerate the formation of higher oxidation states of  $\text{Mn}^{\text{III}}(\text{TPPS})$  in systems containing  $\text{H}_2\text{O}_2$ , PAA and sodium perborate.

**Supplementary Materials:** The following are available online at <http://www.mdpi.com/2073-4344/10/6/610/s1>: Figure S1: Plots of  $k_{\text{obs}}$  versus  $\text{H}_2\text{O}_2$  concentration for the reaction of  $\text{Mn}^{\text{III}}(\text{TPPS})$  with  $\text{H}_2\text{O}_2$  at  $\text{pH} = 9.3$ ; Figure S2: Plots of  $k_{\text{obs}}$  versus  $\text{H}_2\text{O}_2$  concentration for the reaction of  $\text{Mn}^{\text{III}}(\text{TPPS})$  with  $\text{H}_2\text{O}_2$  at  $\text{pH} = 11$ ; Figure S3: Dependence of  $k_{\text{obs}}$  on  $[\text{PAA}]$  for the reaction of  $\text{Mn}^{\text{III}}(\text{TPPS})$  with PAA at  $\text{pH} = 11$ ; Figure S4: Plots of  $k_{\text{obs}}$  versus NaOCl concentration for the reaction of  $\text{Mn}^{\text{III}}(\text{TPPS})$  with  $\text{H}_2\text{O}_2$  at  $\text{pH} = 9.3$ ; Figure S5: Dependence of  $k_{\text{obs}}$  on  $[\text{NaOCl}]$  for the reaction of  $\text{Mn}^{\text{III}}(\text{TPPS})$  with NaOCl at  $\text{pH} = 11$ ; Figure S6: Plots of  $k_{\text{obs}}$  versus persulfate

concentration for the reaction of  $Mn^{III}$ (TPPS) with peroxomonosulfate at pH = 11; Figure S7: Dependence of  $k_{obs}$  on [perborate] for the reaction of  $Mn^{III}$ (TPPS) with perborate at pH = 11.

**Author Contributions:** R.v.E. and M.P. conceived and designed the experiments; M.P. performed the experiments; M.P., R.v.E. and Ł.O. analyzed the data; M.P. and G.S. contributed reagents/materials/analytical tools; M.P., R.v.E., Ł.O. and G.S. wrote the manuscript. All authors have read and agreed to the published version of the manuscript.

**Funding:** This research was funded by the National Science Center in Poland under grant number DEC-2016/21/N/ST4/00172. The APC was funded by the Faculty of Chemistry of the Jagiellonian University in Kraków.

**Acknowledgments:** The Faculty of Chemistry of the Jagiellonian University is the beneficiary of structural funds from the European Union, grant no. POIG. 02.01.00-12-023/08 “Atomic Scale Science for Innovative Economy (ATOMIN)”.

**Conflicts of Interest:** The authors declare no conflict of interest. The founding sponsors had no role in the design of the study; in the collection, analyses, or interpretation of data; in the writing of the manuscript; and in the decision to publish the results.

## References

1. Pearce, C.I.; Lloyd, J.R.; Guthrie, J.T. The removal of colour from textile wastewater using whole bacterial cells: A review. *Dyes Pigment.* **2003**, *58*, 179–196. [[CrossRef](#)]
2. Asghar, A.; Abdul Raman, A.A.; Wan Daud, W.M.A. Advanced oxidation processes for in-situ production of hydrogen peroxide/hydroxyl radical for textile wastewater treatment: A review. *J. Clean. Prod.* **2015**, *87*, 826–838. [[CrossRef](#)]
3. Rajkumar, D.; Kim, J.G. Oxidation of various reactive dyes with in situ electro-generated active chlorine for textile dyeing industry wastewater treatment. *J. Hazard. Mater.* **2006**, *136*, 203–212. [[CrossRef](#)] [[PubMed](#)]
4. Ghodbane, H.; Hamdaoui, O. Intensification of sonochemical decolorization of anthraquinonic dye Acid Blue 25 using carbon tetrachloride. *Ultrason. Sonochem.* **2009**, *16*, 455–461. [[CrossRef](#)]
5. Lin, S.H.; Chen, M.L. Treatment of textile wastewater by chemical methods for reuse. *Water Res.* **1997**, *31*, 868–876. [[CrossRef](#)]
6. Can, O.T.; Kobya, M.; Demirbas, E.; Bayramoglu, M. Treatment of the textile wastewater by combined electrocoagulation. *Chemosphere* **2006**, *62*, 181–187. [[CrossRef](#)]
7. Chen, G. Electrochemical technologies in wastewater treatment. *Sep. Purif. Technol.* **2004**, *38*, 11–41. [[CrossRef](#)]
8. Chang, W.; Hong, S.; Park, J. Effect of zeolite media for the treatment of textile wastewater in a biological aerated filter. *Process Biochem.* **2002**, *37*, 693–698. [[CrossRef](#)]
9. Ellouze, E.; Tahri, N.; Amar, R. Enhancement of textile wastewater treatment process using Nanofiltration. *Desalination* **2012**, *286*, 16–23. [[CrossRef](#)]
10. Jiang, J.; Lloyd, B. Progress in the development and use of ferrate(VI) salt as an oxidant and coagulant for water and wastewater treatment. *Water Res.* **2002**, *36*, 1397–1408. [[CrossRef](#)]
11. Bulc, T.G.; Ojstršek, A. The use of constructed wetland for dye-rich textile wastewater treatment. *J. Hazard. Mater.* **2008**, *155*, 76–82. [[CrossRef](#)] [[PubMed](#)]
12. Lin, S.H.; Peng, C.F. Treatment of textile wastewater by electrochemical method. *Water Res.* **1994**, *28*, 277–282. [[CrossRef](#)]
13. Perkowski, J.; Kos, L.; Ledakowicz, S. Application of Ozone in Textile Wastewater Treatment. *Ozone Sci. Eng.* **1996**, *18*, 73–85. [[CrossRef](#)]
14. Hage, R.; Lienke, A. Applications of Transition-Metal Catalysts to Textile and Wood-Pulp Bleaching. *Angew. Chem. Int. Ed.* **2006**, *45*, 206–222. [[CrossRef](#)] [[PubMed](#)]
15. Bäckvall, J.E. *Modern Oxidation Methods*; WILEY-VCH: Weinheim, Germany, 2010; pp. 371–381.
16. Chatterjee, D.; Ember, E.; Pal, U.; Ghosh, S.; van Eldik, R. Remarkably high catalytic activity of the  $Ru^{III}(\text{edta})/H_2O_2$  system towards degradation of the azo-dye Orange II. *Dalton Trans.* **2011**, *40*, 10473–10480. [[CrossRef](#)]
17. Rothbart, S.; van Eldik, R. Manganese Compounds as Versatile Catalysts for the Oxidative Degradation of Organic Dyes. *Adv. Inorg. Chem.* **2013**, *65*, 165–215. [[CrossRef](#)]

18. Gilbert, B.C.; Lindsay Smith, J.R.; Newton, M.S.; Oakes, J.; Prats, R.P.i. Azo dye oxidation with hydrogen peroxide catalysed by manganese 1,4,7-triazacyclononane complexes in aqueous solutions. *Org. Biomol. Chem.* **2003**, *1*, 1568–1577. [[CrossRef](#)]
19. Zaharia, C.; Suteu, D.; Muresan, A.; Muresan, R.; Popescu, A. Textile wastewater treatment by homogeneous oxidation with hydrogen peroxide. *Environ. Eng. Manag. J.* **2009**, *8*, 1359–1369. [[CrossRef](#)]
20. Pagano, M.; Ciannarella, R.; Locaputo, V.; Mascolo, G.; Volpe, A. Oxidation of azo and anthraquinonic dyes by peroxy monosulphate activated by UV light. *J. Environ. Sci. Health A* **2018**, *53*, 393–404. [[CrossRef](#)]
21. Lin, K.A.; Lin, T. Degradation of Acid Azo Dyes Using Oxone Activated by Cobalt Titanate Perovskite. *Water Air Soil Pollut.* **2017**, *229*, 10. [[CrossRef](#)]
22. Yuan, Z.; Ni, Y.; Van Heiningen, A.R.P. Kinetics of peracetic acid decomposition: Part I: Spontaneous decomposition at typical pulp bleaching conditions. *Can. J. Chem. Eng.* **1997**, *75*, 37–41. [[CrossRef](#)]
23. Emmons, W.D. The Oxidation of Amines with Peracetic Acid. *J. Am. Chem. Soc.* **1957**, *79*, 5528–5530. [[CrossRef](#)]
24. Appels, L.; Assche, A.V.; Willems, K.; Degrève, J.; Van Impe, J.; Dewil, R. Peracetic acid oxidation as an alternative pre-treatment for the anaerobic digestion of waste activated sludge. *Bioresour. Technol.* **2011**, *102*, 4124–4130. [[CrossRef](#)] [[PubMed](#)]
25. Kitis, M. Disinfection of wastewater with peracetic acid: A review. *Environ. Int.* **2004**, *30*, 47–55. [[CrossRef](#)]
26. Wagner, M.; Brumelis, D.; Gehr, R. Disinfection of Wastewater by Hydrogen Peroxide or Peracetic Acid: Development of Procedures for Measurement of Residual Disinfectant and Application to a Physicochemically Treated Municipal Effluent. *Water Environ. Res.* **2002**, *74*, 33–50. [[CrossRef](#)] [[PubMed](#)]
27. Suess, H.U. *Pulp Bleaching Today*; De Gruyter: Berlin, Germany, 2010. [[CrossRef](#)]
28. Zhao, R.; Tang, Y.; Wei, S.J.; Xu, X.; Shi, X.; Zhang, G. Electrosynthesis of sodium hypochlorite in room temperature ionic liquids and in situ electrochemical epoxidation of olefins. *React. Kinet. Mech. Cat.* **2012**, *106*, 37–47. [[CrossRef](#)]
29. Page, P.C.B.; Parker, P.; Buckley, B.R.; Rassias, G.A.; Bethell, D. Organocatalysis of asymmetric epoxidation by iminium salts using sodium hypochlorite as the stoichiometric oxidant. *Tetrahedron* **2009**, *65*, 2910–2915. [[CrossRef](#)]
30. Kirihaara, M.; Okada, T.; Sugiyama, Y.; Akiyoshi, M.; Matsunaga, T.; Kimura, Y. Sodium Hypochlorite Pentahydrate Crystals (NaOCl·5H<sub>2</sub>O): A Convenient and Environmentally Benign Oxidant for Organic Synthesis. *Org. Process Res. Dev.* **2017**, *21*, 1925–1937. [[CrossRef](#)]
31. Zhang, W.; Jacobsen, E.N. Asymmetric olefin epoxidation with sodium hypochlorite catalyzed by easily prepared chiral manganese(III) salen complexes. *J. Org. Chem.* **1991**, *56*, 2296–2298. [[CrossRef](#)]
32. Gonsalvi, L.; Arends, I.W.C.E.; Moilanen, P.; Sheldon, R.A. The Effect of pH Control on the Selective Ruthenium-Catalyzed Oxidation of Ethers and Alcohols with Sodium Hypochlorite. *Adv. Synth. Catal.* **2003**, *345*, 1321–1328. [[CrossRef](#)]
33. Chellamani, A.; Harikengaram, S. Mechanism of oxidation of aryl methyl sulfoxides with sodium hypochlorite catalyzed by (salen)Mn(III) complexes. *J. Mol. Catal. A Chem.* **2006**, *247*, 260–267. [[CrossRef](#)]
34. Chellamani, A.; Harikengaram, S. Mechanism of (Salen)manganese(III)-Catalyzed Oxidation of Aryl Phenyl Sulfides with Sodium Hypochlorite. *Helv. Chim. Acta* **2011**, *94*, 453–463. [[CrossRef](#)]
35. Zhang, Y.; Zhou, Q.; Ma, W.; Zhao, J. Enantioselective oxidation of racemic secondary alcohols catalyzed by chiral Mn(III)-salen complex with sodium hypochlorite as oxidant. *Catal. Commun.* **2014**, *45*, 114–117. [[CrossRef](#)]
36. Patil, R.D.; Sasson, Y. Naphthalenes Oxidation by Aqueous Sodium Hypochlorite Catalyzed by Ruthenium Salts Under Phase-Transfer Catalytic Conditions. *Catal. Lett.* **2016**, *146*, 991–997. [[CrossRef](#)]
37. Mirkhani, V.; Tangestaninejad, S.; Moghadam, M.; Yadollahi, B. Efficient and selective epoxidation of alkenes by supported manganese porphyrin under ultrasonic irradiation. *J. Chem. Res.* **2000**, *2000*, 515–517. [[CrossRef](#)]
38. Tangestaninejad, S.; Moghadam, M.; Mirkhani, V.; Mohammadpoor-Baltork, I.; Hoseini, N. Efficient and Selective Hydrocarbon Oxidation with Sodium Periodate Catalyzed by Supported Manganese(III) Porphyrin. *J. Iran. Chem. Soc.* **2010**, *7*, 663–672. [[CrossRef](#)]
39. Zakavi, S.; Ebadi, S.; Javanmard, M. Nanosized cationic and anionic manganese porphyrins as mesoporous catalysts for the oxidation of olefins: Nano versus bulk aggregates. *Appl. Organomet. Chem.* **2018**, *32*, e4175. [[CrossRef](#)]

40. Song, R.; Sorokin, A.; Bernadou, J.; Meunier, B. Metalloporphyrin-Catalyzed Oxidation of 2-Methylnaphthalene to Vitamin K<sub>3</sub> and 6-Methyl-1,4-naphthoquinone by Potassium Monopersulfate in Aqueous Solution. *J. Org. Chem.* **1997**, *62*, 673–678. [[CrossRef](#)]
41. Prochner, M.; Orzeł, Ł.; Stochel, G.; van Eldik, R. Spectroscopic and kinetic evidence for redox cycling, catalase and degradation activities of MnIII(TPPS) in a basic aqueous peroxide medium. *Chem. Commun.* **2016**, *52*, 5297–5300. [[CrossRef](#)]
42. Prochner, M.; Orzeł, Ł.; Stochel, G.; van Eldik, R. Catalytic Degradation of Orange II by MnIII(TPPS) in Basic Hydrogen Peroxide Medium: A Detailed Kinetic Analysis. *Eur. J. Inorg. Chem.* **2018**, *2018*, 3462–3471. [[CrossRef](#)]
43. Arasasingham, R.D.; He, G.X.; Bruice, T.C. Mechanism of manganese porphyrin-catalyzed oxidation of alkenes. Role of manganese(IV)-oxo species. *J. Am. Chem. Soc.* **1993**, *115*, 7985–7991. [[CrossRef](#)]
44. Nam, W.; Kim, I.; Lim, M.H.; Choi, H.J.; Lee, J.S.; Jang, H.G. Isolation of an oxomanganese(v) porphyrin intermediate in the reaction of a manganese(III) porphyrin complex and H<sub>2</sub>O<sub>2</sub> in aqueous solution. *Chem.-Eur. J.* **2002**, *8*, 2067–2071. [[CrossRef](#)]
45. Lahaye, T.; Groves, J.T. Modeling the haloperoxidases: Reversible oxygen atom transfer between bromide ion and an oxo-Mn(V) porphyrin. *J. Inorg. Biochem.* **2007**, *101*, 1786–1797. [[CrossRef](#)] [[PubMed](#)]
46. Ember, E.; Rothbart, S.; Puchta, R.; van Eldik, R. Metal ion-catalyzed oxidative degradation of Orange II by H<sub>2</sub>O<sub>2</sub>. High catalytic activity of simple manganese salts. *New J. Chem.* **2009**, *33*, 34–49. [[CrossRef](#)]
47. Rothbart, S.; Ember, E.; van Eldik, R. Comparative study of the catalytic activity of [Mn<sup>II</sup>(bpy)<sub>2</sub>Cl<sub>2</sub>] and [Mn<sup>III/IV</sup>(μ-O)<sub>2</sub>(bpy)<sub>4</sub>](ClO<sub>4</sub>)<sub>3</sub> in the H<sub>2</sub>O<sub>2</sub> induced oxidation of organic dyes in carbonate buffered aqueous solution. *Dalton Trans.* **2010**, *39*, 3264–3272. [[CrossRef](#)]
48. Richardson, D.E.; Yao, H.; Frank, K.M.; Bennett, D.A. Equilibria, Kinetics, and Mechanism in the Bicarbonate Activation of Hydrogen Peroxide: Oxidation of Sulfides by Peroxymonocarbonate. *J. Am. Chem. Soc.* **2000**, *122*, 1729–1739. [[CrossRef](#)]
49. Bakhmutova-Albert, E.V.; Yao, H.; Denevan, D.E.; Richardson, D.E. Kinetics and mechanism of peroxymonocarbonate formation. *Inorg. Chem.* **2010**, *49*, 11287–11296. [[CrossRef](#)]
50. Swern, D. *Organic Peroxides*; Wiley: New York, NY, USA, 1970; Volume I. [[CrossRef](#)]
51. Rothbart, S.; Ember, E.; van Eldik, R. Mechanistic studies on the oxidative degradation of Orange II by peracetic acid catalyzed by simple manganese(ii) salts. Tuning the lifetime of the catalyst. *New J. Chem.* **2012**, *36*, 732–748. [[CrossRef](#)]
52. Evans, D.F.; Upton, M.W. Studies on singlet oxygen in aqueous solution. Part 3. The decomposition of peroxy-acids. *J. Chem. Soc. Dalton Trans.* **1985**, 1151–1153. [[CrossRef](#)]
53. Koubek, E.; Hagggett, M.L.; Battaglia, C.J.; Ibne-Rasa, K.M.; Pyun, H.Y.; Edwards, J.O. Kinetics and Mechanism of the Spontaneous Decompositions of Some Peroxoacids, Hydrogen Peroxide and t-Butyl Hydroperoxide. *J. Am. Chem. Soc.* **1963**, *85*, 2263–2268. [[CrossRef](#)]
54. Ball, D.L.; Edwards, J.O. The Kinetics and Mechanism of the Decomposition of Caro's Acid. I. *J. Am. Chem. Soc.* **1956**, *78*, 1125–1129. [[CrossRef](#)]
55. Awad, M.I.; Harnood, C.; Tokuda, K.; Ohsaka, T. Simultaneous Electroanalysis of Peroxyacetic Acid and Hydrogen Peroxide. *Anal. Chem.* **2001**, *73*, 1839–1843. [[CrossRef](#)]
56. Urano, H.; Fukuzaki, S. The Mode of Action of Sodium Hypochlorite in the Decolorization of Azo Dye Orange II in Aqueous Solution. *Biocontrol Sci.* **2011**, *16*, 123–126. [[CrossRef](#)] [[PubMed](#)]
57. Morris, J.C. The acid ionization constant of HOCl from 5 to 35. *J. Phys. Chem.* **1966**, *70*, 3798–3805. [[CrossRef](#)]
58. Lister, M.W. Decomposition of sodium hypochlorite: The uncatalyzed reaction. *Can. J. Chem.* **1956**, *34*, 465–478. [[CrossRef](#)]
59. Zheng, T.; Richardson, D.E. Homogeneous aqueous oxidation of organic molecules by Oxone<sup>®</sup> and catalysis by a water-soluble manganese porphyrin complex. *Tetrahedron Lett.* **1995**, *36*, 833–836. [[CrossRef](#)]
60. Ghanbari, F.; Moradi, M. Application of peroxymonosulfate and its activation methods for degradation of environmental organic pollutants: Review. *Chem. Eng. J.* **2017**, *310*, 41–62. [[CrossRef](#)]
61. Durrant, M.C.; Davies, D.M.; Deary, M.E. Dioxaborirane: A highly reactive peroxide that is the likely intermediate in borate catalysed electrophilic reactions of hydrogen peroxide in alkaline aqueous solution. *Org. Biomol. Chem.* **2011**, *9*, 7249–7254. [[CrossRef](#)]
62. Pizer, R.; Tihal, C. Peroxoborates. Interaction of boric acid and hydrogen peroxide in aqueous solution. *Inorg. Chem.* **1987**, *26*, 3639–3642. [[CrossRef](#)]

63. Deary, M.E.; Durrant, M.C.; Davies, D.M. A kinetic and theoretical study of the borate catalysed reactions of hydrogen peroxide: The role of dioxaborirane as the catalytic intermediate for a wide range of substrates. *Org. Biomol. Chem.* **2013**, *11*, 309–317. [[CrossRef](#)]
64. Davies, D.M.; Deary, M.E.; Quill, K.; Smith, R.A. Borate-Catalyzed Reactions of Hydrogen Peroxide: Kinetics and Mechanism of the Oxidation of Organic Sulfides by Peroxoborates. *Chem. Eur. J.* **2005**, *11*, 3552–3558. [[CrossRef](#)] [[PubMed](#)]



© 2020 by the authors. Licensee MDPI, Basel, Switzerland. This article is an open access article distributed under the terms and conditions of the Creative Commons Attribution (CC BY) license (<http://creativecommons.org/licenses/by/4.0/>).